Space Interferometry Mission Instrument Mechanical Layout[1]

Kim M. Aaron
California Institute of Technology, Jet Propulsion Laboratory
4800 Oak Grove Drive
Pasadena, CA 91109
(818) 354-2816
Kim.M.Aaron@jpl.nasa.gov

David M. Stubbs
Lockheed Martin Missiles & Space
Dept L9-23, Bldg 201
3251 Hanover Street
Palo Alto, CA 94304
(650) 424-2365
david.stubbs@lmco.com

Keith Kroening
TRW
1 Space Park R9/2078
Redondo Beach, California 90278
(310) 814-7433
keith.kroening@trw.com

Abstract—The Space Interferometry Mission, planned for launch in 2006, will measure the positions of celestial objects to an unprecedented accuracy of 4×10^{-6} arc sec (about 1 billionth of a degree). In order to achieve this accuracy, which represents an improvement of almost two orders of magnitude over previous astrometric measurements, a ten-meter baseline interferometer will be flown in space. Starlight is collected by 33 cm diameter telescopes and combined to form fringes on detectors. To achieve the stated accuracy, the position of these fringes must be measured to a fraction of a wavelength of visible light. Passive vibration isolation and several layers of active control are used to stabilize the starlight wavefronts at sub-nanometer levels. Tight thermal control is coupled with very low CTE materials. Certain parts of the instrument need to be stabilized so that they move more slowly than the speed at which a baby grows.

TABLE OF CONTENTS

1. INTRODUCTION

This paper focuses on the mechanical layout of the single main instrument of the Space Interferometry Mission (SIM). The Space Interferometry Mission Instrument consists of four major subsystems: Starlight (STL), Metrology (MET), Precision Support Structure (PSS) and Real Time Control (RTC). RTC will not be covered since this paper is focusing on the mechanical configuration of the instrument, not the controls.

After a brief overview and discussion of the major requirements, the Starlight and Metrology Subsystems will be discussed. These constitute the major optical elements of the instrument. Following these sections, the foundation upon which everything is mounted, the Precision Support Structure (PSS), will be described along with some important thermal and vibrational aspects which constitute disturbance sources that must be rejected in part by the PSS.

JPL and the SIM Industry Partners are responsible for different subsystems. JPL is responsible for RTC, TRW for PSS, and Lockheed Martin for STL and MET. Each subsystem delivers flight hardware to the program and deals with a plethora of inter-subsystem interfaces. Due to the stringent thermal and structural dynamic constraints,

[1] 0-7803-5846-5/00/$10.00 © 2000 IEEE

Graphite Cyanoacrylate (GrCy) is a likely choice of composite material for all precision structures.

Figure 1 Space Interferometry Mission (SIM) Flight System Painting

The instrument operates by collecting starlight using pairs of small telescopes and combining the light onto sensitive CCD detectors to create constructive interference. When all elements are carefully aligned, very precise measurements using a laser interferometric metrology system, coupled with knowledge of guide star locations, can be used to establish the angular position of the target star or other celestial object. To achieve micro arc second (μas) accuracy, the laser metrology system must have a precision of about a hundred picometers (about an angstrom: 10^{-10} m). This is many times smaller than the size of a hydrogen atom. This measurement is an average across the metrology laser beam, and does not refer to the position of a physical point.

Most of the traditional spacecraft subsystems are isolated from the very large single instrument. The optical elements are all mounted to a precision structure, which is physically decoupled from the spacecraft bus by vibration isolators. The spacecraft engineering subsystems are located in a structure, which we refer to as a "backpack." There are two backpacks mounted beneath the wings of the PSS. The second backpack houses a major share of the real-time control electronics (instrument-specific electronics which do not need to be in close proximity to elements they are controlling). Other portions of the RTC must be mounted close to high bandwidth actuators and sensors to avoid latency issues. The positions of key optical elements are controlled based on measurements using interferometric laser metrology gauges. The general layout of the flight system is designed to minimize the magnitude of and reduce the effects of unavoidable disturbances. A more in-depth overview is given in a companion paper by Peter Kahn at this same conference [1]. An artist's rendering of the SIM flight system, by Phil Weisgerber, is shown in figure 1.

2. REQUIREMENTS

From the top-level science requirements, lower level requirements have been derived to enable the conceptual design effort to proceed. With a ten-meter baseline, an error of 1 μas corresponds to an error of 48.5 picometers in the baseline length. A single measurement accuracy of 7.5 μas yields a total error budget of 364 pm (3.64 Å). An error budget has been developed to allocate this error among various contributions. This error budget imposes stringent requirements on many elements of SIM. Top level science

requirements are shown in table 1. Derived requirements applying to the instrument are shown in table 2.

Table 1 Science Requirements (Tentative)

Overall System Science Requirements		
The visible observational bandwidth	0.4 - 0.9	μm
Target accessibility	≥6	months
Sky coverage within a year	4π	steradian
Mission lifetime (from end of verification phase)	5	years
The minimum continuous viewing period	10	minutes
The target of opportunity response	≤4	days
Wide Angle Astrometry Science Requirements		
Field of regard	≥15	degree
Single observation astrometric accuracy	4	μas
Overall mission astrometric and parallax accuracy	4	μas
Minimum star brightness	20	Visual magnitude
Proper motion accuracy	2	μas/year
Narrow Angle Astrometry Science Requirements		
Field of regard	1	degrees
Single observation astrometric accuracy	1	μas
Minimum star brightness	20	Visual magnitude
Proper motion accuracy	1	μas/year
Imaging Science (including Nulling-Imaging)		
Continuum sensitivity (averaged over 300 nm bandwidth)	0.6	mJ/year
Emission line sensitivity (integrated in 4 nm channel bandwidth)	2.5×10^{-14}	erg/cm^2/s
Image dynamic range	100:1	
Spectral Coverage	500- 1000	nm
Spectral Resolution	160	$(\lambda/\Delta\lambda)$
Largest baseline	10	m
Shortest baseline	≤1	m
Baseline increment	≤1	m
Number of independent observed (u, v) points	150	
Total observing time	≥10	hr
Fringe amplitude calibration consistency	1	%
Fringe phase calibration consistency	8	degree
Number of imaging target fields	50	
Nulling Requirements		
Visual achromatic null over 20% spectrum	1×10^{-4}	
Null stability	10	%
Null stability duration	10	sec

Table 2 Selected Derived Requirements

Starlight Requirements		
Entrance Pupil	33	cm
Entrance Pupil area used for Starlight	50	%
Starlight Diameter Compression Ratio	11:1	
Throughput (photons detected/photon incident)	0.6	
Throughput mismatch (arm to arm)	<10	%
Telescope Field of Regard	15	degree
Starlight Interferometric Visibility	0.78	
Polarization mismatch between arms	<10	degree
Optical Element Wavefront Quality	λ/100 rms	
Pathlength Difference between arms	10	micron
Angular offset between chief rays of arms	<40	mas
Siderostat Pointing Actuator accuracy	50	mas
Metrology Requirements		
Baseline Measurement Precision		
Two-week stability (grid campaign)	100	pm
One-hour stablility (wide angle astrometry)	70	pm
Five-minute stability (narrow angle astrometry)	45	pm

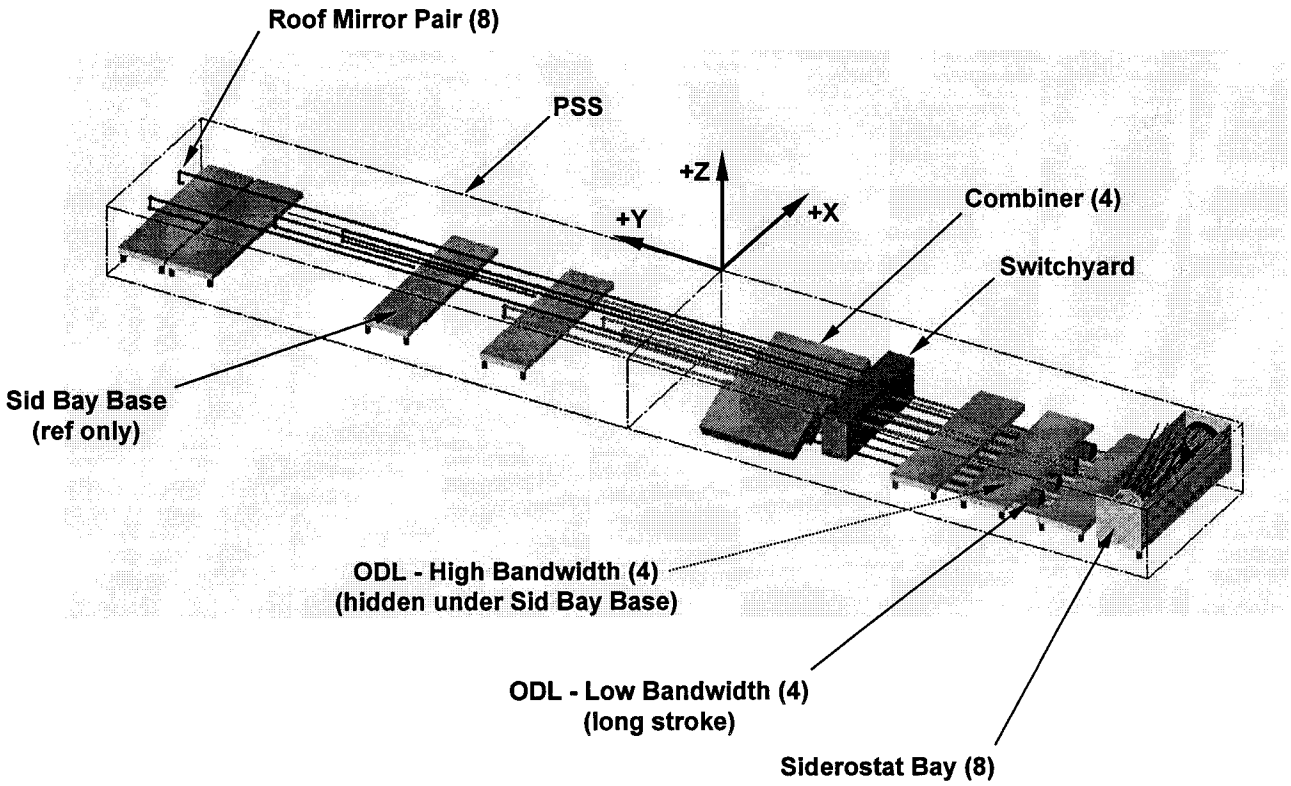

Figure 2 Instrument Layout

3. STARLIGHT SUBSYSTEM

The Starlight Subsystem consists of eight Siderostat Bays, eight Roof Mirror assemblies, a Switchyard, four Low Bandwidth Optical Delay Lines (Low ODL), four High Bandwidth Optical Delay Lines (High ODL) and four Beam Combiners. See figure 2.

Each Siderostat Bay contains a 2-axis Siderostat Mirror Gimbal (Az/El), a 33 cm aperture off-axis Beam Compressor, a Fast Steering Mirror Beamsplitter (FSM), a Coarse Acquisition Camera, and several alignment mechanisms. See figure 3. The Siderostat Gimbal must cover a conical Field-of-Regard (FOR) of 15 degrees, be capable of auto-collimation with the Compressor for on-orbit calibration and have the ability to move several millimeters fore and aft to align the eight Siderostat Mirrors. The Compressor is an off-axis, 11:1 telescope consisting of an f/1.5 parent parabolic Primary Mirror and a secondary mirror. The starlight is focussed to a point between the primary and secondary mirrors. A field stop with a tiny hole is mounted at this focal point to pass the starlight, while rejecting off-axis stray light. This arrangement also allows both powered optics to be concave mirrors, which are easier to polish than convex mirrors. The Compressor wavefront quality is $\lambda/25$ rms at 0.633 microns.

The challenging picometer-level optical requirements impose stringent thermal and structural dynamic requirements on the Starlight system in addition to optical surface quality. Optics (all are $\lambda/100$ rms wavefront) must be maintained to within tens of millikelvins (mK). To meet this requirement, each optic must either be housed within a mK-controlled enclosure or have its own radiatively-coupled heater plate. The Siderostat and Collector Primary Mirrors each have a heater plate radiating to its entire back and side surfaces to reduce and maintain stable gradients within the mirrors. The heater plate back and sides are enclosed in multi-layer insulation (MLI).

The Roof Mirror assemblies consist of two plano mirrors at ninety degrees to each other. Their positions are fixed to provide identical path lengths from each Siderostat Mirror to the first mirror in the Switchyard and to arrange for the Starlight beams from each Siderostat to enter the Switchyard from the same side (preserving polarization). See figures 2 and 4 for placement.

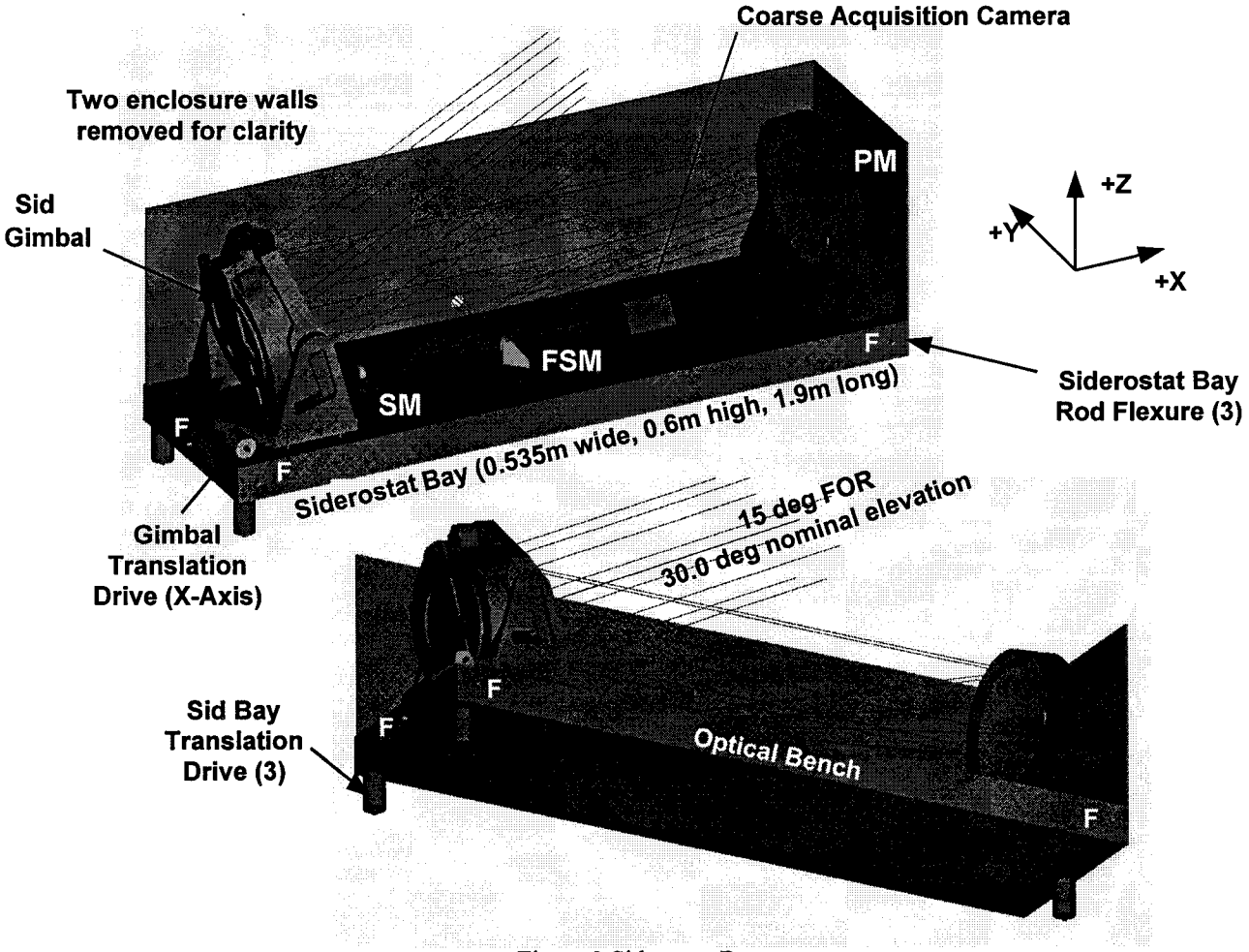

Figure 3 Siderostat Bay

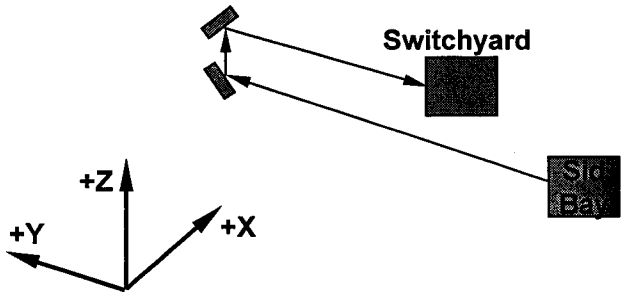

1. All beams exit Sid Bays in +Y direction.
2. 180 deg reversal at Roof Mirror pairs.
3. Enter Switchyard with identical OPDs.

Figure 4 Beam Path: Siderostat Bay(s) - Switchyard

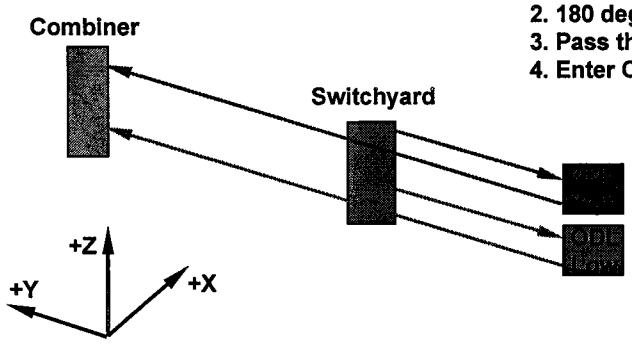

1. All beams exit Switchyard in -Y direction.
2. 180 deg reversal at ODLs, correcting baseline OPDs.
3. Pass through Switchyard beam clearance holes.
4. Enter Combiner.

Figure 5 Beam Path: Switchyard - Combiner

The Switchyard has eight light paths entering from each of the Siderostat Bays and eight paths exiting. The Switchyard allows any combination of two Siderostat Bays to attain interferometer baselines. Not only does this arrangement allow many baseline lengths from 0.6m to 10.0m (useful for synthetic aperture imaging), but it also adds redundancy should one or two Siderostat Bays fail for any reason. See figure 5. Polarization and pupil rotation must be identical within both legs of an Interferometer. Using two simple plano mirrors to form the periscope connecting incoming beams to outgoing beams does not preserve polarization. One of the rotary devices can be a plano mirror but the other must use a three-mirror Porro assembly. These three mirrors generate a 90 degree beam path change just as a single mirror would, but the overall combination of four mirrors maintains polarization as required.

The eight light paths exiting the Switchyard are in pairs. One beam goes to a Low Bandwidth ODL while the other goes to a High Bandwidth ODL. The Low ODL is an optical Catseye that travels up to 1.5 meters to compensate for 3.0 meters maximum required delay due to the angle changes of the Siderostat Mirror. The High ODL is also a Catseye but it takes out mid and high bandwidth path length errors caused by vibration and beam walk errors.

The beam path then enters the last optical assembly within Starlight: the Beam Combiner. The Combiner takes the two, 3 cm diameter beam paths from two different Siderostat Bays, combines them using a beam splitter in reverse, then relays the interfered beam onto two CCD Camera focal planes, a Fringe Tracker Camera and an Angle Tracker Camera. The Combiner is currently in the conceptual phase.

Each Siderostat Bay is mounted to the PSS using flexures and three actuators, allowing for on-orbit alignment of all the Siderostat Bays. Pointing and positional stability of the Siderostat Bays within the PSS is to tens of milliradians and tens of microns, respectively. Knowledge of the Siderostat positions is required down to a few tens of picometers (averaged across the starlight wavefront) to attain the required astrometric measurement precision. The diameter of a hydrogen atom is approximately one hundred picometers. The Metrology Subsystem (MET) provides these measurements.

4. METROLOGY SUBSYSTEM

The Metrology Subsystem (MET) is used to measure very precisely the locations of the eight siderostats with respect to one another as well as to measure the distance traveled by starlight from the sidersostat mirrors all the way through the system to a point very close to the detectors inside the beam combiners.

MET consists of internal and external metrology. Internal MET measures distances between the beam combiner corner cubes and the siderostat corner cubes using super-

precision retro-reflecting corner cubes (λ/5000) and Beam Launchers. The Beam Launchers (currently conceptual) are situated between the two corner cubes and aim a laser beam along a direction connecting the vertices of both corner cubes to measure the distance between these two fiducial points. There are eight internal metrology Beam Launchers mounted two per Beam Combiner just ahead of the point at which the starlight beams are combined.

External MET measures distances between the Siderostat Mirror corner cubes and the Corner Cubes of the Metrology Kite mounted on the end of a boom protruding from the precision structure. External MET also measure distances between each of the corner cubes of the metrology kite. See figure 6.

The Kite has four corners, each with a triple corner cube, allowing measurements among the corners and to each Siderostat Bay. See figure 7. A triple corner cube is an assembly of mirrors arranged to form three different retro-reflecting corners with the vertex of each corner at the same location (within about 1 μm). Each of the eight Siderostat Bays contains four MET Beam Launchers, allowing measurement to each of the four Kite corners. These Beam Launchers, mounted on tip/tilt piezo gimbals, are each in-line with the Siderostat Mirror Corner Cube and one of the four Kite corners. There are four Beam Launchers per Siderostat Bay. Six more Beam Launchers are mounted on the Kite. The Kite exists just to measure the positions of the siderostat mirrors with respect to one another. Effectively, three-dimensional triangulation is used to locate the siderostats with respect to the Kite.

The laser is generated using a highly stable reference cavity and is fed to the 46 various beam launchers using optical fibers and a network of splitters. The beam is diverted towards the corner cubes using polarizing beam splitter cubes. The beam makes a complete round trip between the two corner cubes and returns to the beam launcher at which point it is combined with a second thermally compensating reference laser beam. Interference fringes between the two beams are counted to determine changes in separation between the two corner cubes. The two lasers are slightly offset in wavelength and used in a heterodyne fashion.

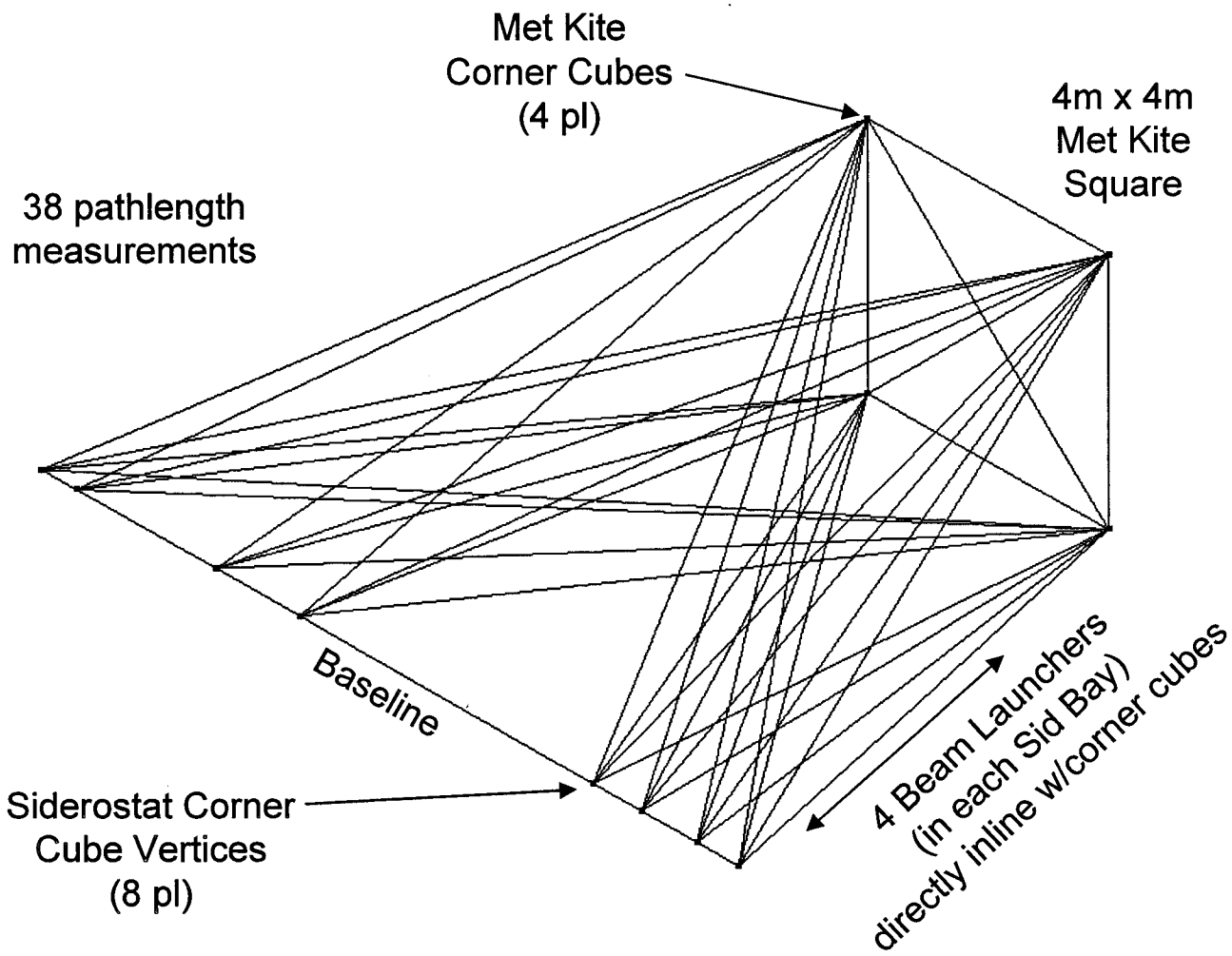

Figure 6 Metrology Kite

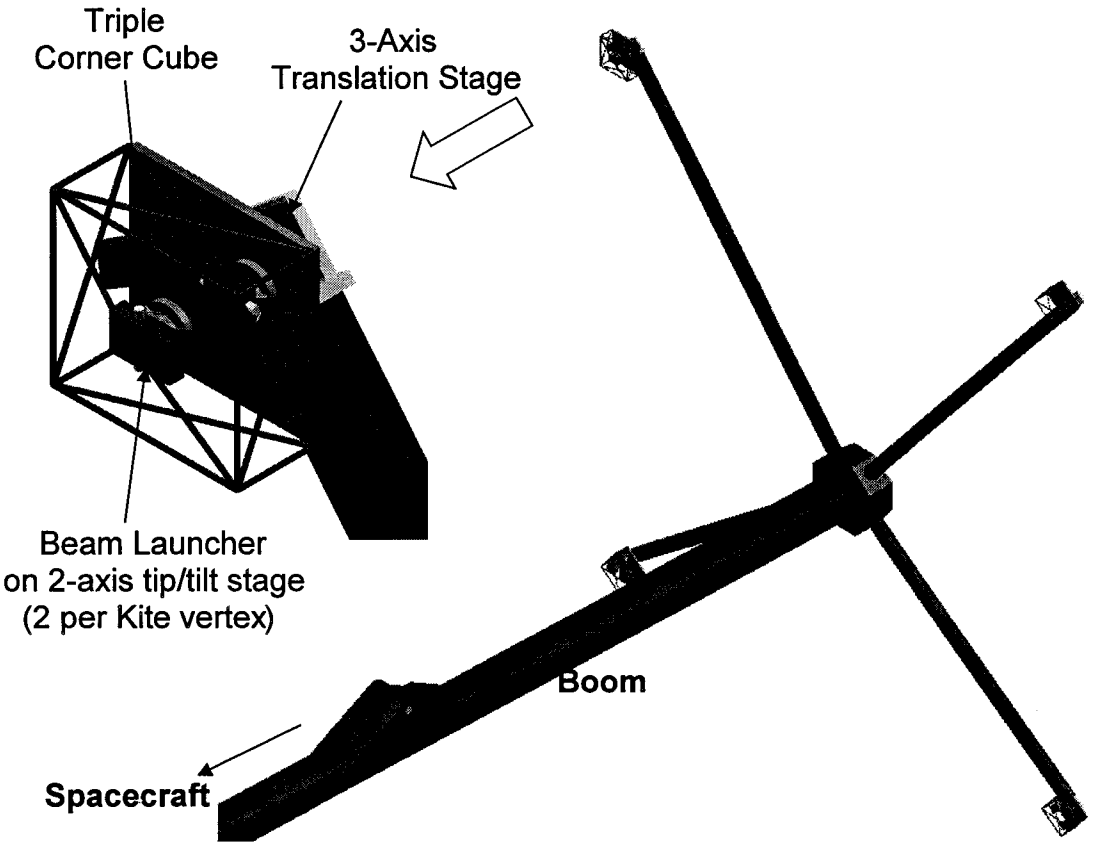

Figure 7 Kite Vertices

5. Precision Support Structure

The goal for the PSS development is to design, build, and validate a structure with minimal thermal distortions (i.e. near zero CTE) and appropriate dynamic response to maintain instrument performance and, where possible, to increase scientific performance or reduce interferometry challenges. The performance requirements will be developed via top down error budget allocation, which trades instrument and structural parameters to maximize the science per dollar. Cost effective development testing will provide key design parameters as well as verify that components can achieve their allocation. These dual use tests will also be used to validate analytic models providing sufficient overlap between tests to assure success.

The baseline PSS designs employ two deployable 'wing' sections to achieve the baseline lengths required to meet the science goals. These wings support the optical elements of the instrument. Each wing will rotate, from its stowed position, about a fixed hinge axis that incorporates a loose fitting pin. When deployed the root section of the wing will engage latch assemblies mounted on the adjacent structure. Mating cup / cone interfaces will assure the alignment of the wing and provide stability once deployed. The initial deployment accuracy would be on the order of ±0.5 cm or less for an overall wingspan of 11+ meters. This approach will allow precision alignment without requiring complex high precision mechanisms as the cup / cone interface would define final positions not the hinge itself. These positioning latches must be evaluated for dynamic and microdynamic effects during component level development testing but the hinge itself can be developed later in the program to reduce Formulation Phase costs. Although the PSS structure will be constructed using lightweight GFRP materials and adhesive-bonded joints, weight optimization is a major design driver. Trade studies will determine the most efficient material design to satisfy system performance with acceptable cost and technical risk.

Dimensional stability and predictability is a critical driver for the PSS. Once deployed the PSS must maintain the instrument alignment within design parameters. Proper selection of the fiber/resin material system, laminate lay-up and manufacturing approach will determine the ability to satisfy system requirements. Previous efforts at Composite Optics Incorporated (COI) have determined that a (0/±45/90) quasi-isotropic lay-up of M55J/954-3 GFRP is a material that can achieve a nominal zero CTE. The 954-3 polycyanate resin system used has desirable characteristics of low outgassing, low moisture absorption, improved micro-crack resistance under thermal cycle conditions, and excellent resistance to space environmental effects. Possibly more important than CTE is CTE variability. COI has

determined that the 'rotate and fold' ply layup technique can control the CTE to the $2x10^{-7}$/K in a flat panel design so a flat panel based structure may be the most controllable.

COI has developed a low cost GFRP tooling approach that minimizes CTE mismatch between part and forming tool which reduces the prestress typically generated in the composite post-cure cool down. This helps ensure high quality, flat details which can be assembled in a room temperature secondary bonding operation to build-up large structures with minimal initial prestress. Metallic coatings have been used to adjust or "tune" the CTE of GFRP on previous programs. The metallic plating process provides an effective barrier to moisture absorption and thereby decreases moisture-related distortions. The effect of moisture absorption/desorption on the dimensional response of polymeric composite materials is well understood. The effect of moisture on a laminate can be many times greater than the effect of a wide temperature change for a space structure but usually occur on the time scale of weeks.

A number of ways to prevent, or compensate for, moisture-induced dimensional instability have been utilized on previous programs. These methods include adjustable optics, optics locations preset to compensate in advance for the hydro-strain motion, use of a "bakeout" procedure and controlled environment and use of a moisture barrier. Recent advances in new hydrophobic resin systems have offered designers an alternative solution to the hydro-strain problem. Moisture will still absorb and desorb from these systems through the barrier, though the strain response is significantly reduced. The degree of effectiveness of the barrier is usually directly related to the material type and thickness being applied (i.e. the thicker the barrier, the more effective it will be).

To ensure that performance requirements are satisfied within cost and schedule constraints, a development effort is necessary for early technical risk retirement. Historically, the most cost-effective means for developing advanced composite structures has been extensive use of test articles with various levels of complexity to mitigate schedule, cost, and technical risk. Tests are structured to provide early input to evolving design, analytic, and manufacturing efforts. Material coupons generate thermoelastic properties and statistical strength allowables. Structural joint strength and stiffness characteristics can also be empirically determined in a cost-effective manner at the coupon level. Past experience at TRW has shown that these coupon data can be incorporated into analytic models to yield accurate predictions for thermal, static, and dynamic structure performance.

Larger test elements will be fabricated to characterize key PSS features such as the wing hinge/latch. The Sub-Structural Test Article (SSTA) is a subsection of the PSS consisting of the key joint area of the PSS wing as seen in figure 8. This figure illustrates the SSTA as conceived for an earlier SIM configuration. The SSTA will be revised to match the current configuration. The SSTA will be tested for dynamic damping/transmissibility, thermal control and stability and microdynamics. The structure utilizes flight materials and construction techniques by our PSS subcontractor, COI. Brassboard level hinges and latches will be installed later at TRW to match form, fit and function for the flight mechanisms. Thermal control subsystem heaters and blankets will be installed for PSS thermal performance testing. The suitability of the thermal design may be verified by thermal vacuum testing of the SSTA. This test will measure quasi-static temperature gradients and provide design sensitivities. The results of this test in conjunction with 'in air' tests of the flight PSS will verify that measured thermal distortion levels are not larger than predicted. This will reduce cost and schedule risk in the development of the

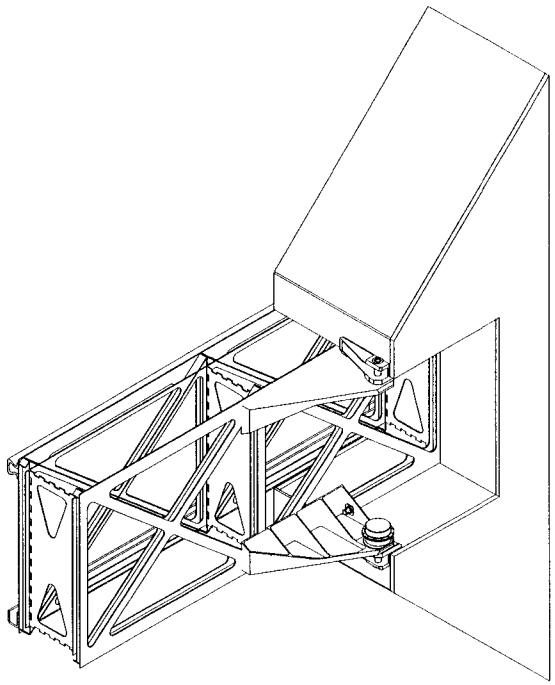

Figure 8 Sub-Structural Test Article

flight PSS structure and thermal control system.

A modal survey will be performed on the PSS in the stowed configuration. Together with sub component modal surveys a free-free model will be developed analytically. The test configuration dynamic model will be correlated to match measured frequencies, mode shapes and damping values. Addition of on-orbit mass to the model will provide confirmation of the on-orbit minimum frequency. Additional transmissibility tests between spacecraft attachment points and optical mounts will be used to provide further refinement of the dynamic model. The test verified dynamic model would then be used to predict on-orbit stability using transmitted reaction wheel and other on orbit disturbances. The isolated wheel disturbances will be available from prior isolation tests run at the unit level.
Microdynamics levels will be measured by subjecting the suspended PSS to thermal transients in a quiet acoustic environment. Ultrasensitive yet low-cost geophones will be placed at optical mounts and monitored for evidence of microdynamics in latches or structure as thermal deformations occur. The geophones give direct measurement of velocity, and a single integration gives displacement. Tests at TRW indicate that ambient vibration levels below the dynamic stability requirement can be met using simple air isolation.

Material coupon tests will be performed to evaluate material properties, lay-ups, and the ability to achieve required CTE levels. Material data will be incorporated into the flight structural and dynamics models. Foundation material coupon tests generate thermoplastic properties and statistical strength allowables. In addition, a substantial test database for bonded GFRP joints already exists but must be verified for microdynamic effects. Dimensional stability properties of the flight GFRP components will be verified by measuring tag end coupons taken directly from the parts. While significant testing has been conducted into controlling the CTE of composite materials via (a) material uniformity, (b) tight process controls, and (c) fabrication techniques, additional CTE testing of large scale flat panels should be conducted. Results of these tests will provide valuable information relative to how accurately the CTE may be controlled over large surface areas using current processing techniques or whether laminate thickness and ply angle deviations affect CTE and therefore the manufacturing process control.

Verification of the flight PSS performance starts during the fabrication and assembly of the PSS wings and central support structure at COI. Process control and inspection is used to assure fabrication and assembly meets process requirements. After bake-out, verification of the thermal distortion properties of the completed structural elements is determined by in-air measurement of distortion with temperature variations. In parallel, TRW will be performing proto-qualification of the PSS mechanisms including load and torque/θ (load/angle) tests will be performed. TRW will then integrate fittings, latches, hinges, deployment mechanisms, harnessing, and heaters/MLI onto the COI structural elements to build up the completed PSS. After bake-out of the MLI and harnessing the dynamic performance of the PSS will be verified by performing large-angle deployment and latch-up tests and then a modal survey of the completed PSS assembly.

After inspection and cleaning, the PSS is transferred to thermal-vacuum for performance verification. The PSS is fitted with distortion/temperature instrumentation to verify thermal balance/distortion in vacuum. After final inspection and cleaning, the PSS is shipped to the JPL/Lockheed Martin team for integration with the instrument assemblies. After return of the integrated instrument to TRW for integration with the spacecraft, the performance of the PSS and Thermal Control Cubsystem (TCS) is indirectly verified during instrument and spacecraft functional tests. Final PSS/TCS performance verification is performed during space vehicle thermal vacuum testing.

6. KEY THERMAL ISSUES

Interferometer optical assemblies and the Precision Support Structure (PSS) have very tight thermal stability requirements. Current estimates for optical components indicate temperature variations are limited to several millikelvin over a one-hour observation sequence. The PSS thermal stability requirement has been estimated at 0.5 C for an aggregate CTE of 0.1×10^{-6}/K. Potential thermal disturbance to these subsystems include time-varying sun angles, on/off heater operation, optical element position changes (slewing), heat pulses from cameras or actuators, and power variations in electronics units.

The design approach to achieving thermal stability is to employ an enclosure that provides a stable radiative environment to surround the controlled assemblies. These thermal enclosures consist of multiple lightweight computer-controlled heater plates and multi-layer insulation blankets (MLI). This thermal design cold-biases the assemblies by using exterior surface components that are always colder than the desired operating temperature, even in direct sunlight. For the required 5-year life, the cold-biasing objective can be achieved by using MLI with silvered-Teflon outer coversheets, whose development TRW pioneered on the Chandra Observatory program. Heaters are controlled using the spacecraft computer which sends on/off commands to the Heater Drive Electronics (HDE), which utilize solid-state switching to turn power on and off to heater plates. Solid-state switching of heaters alleviates concerns about microdynamic excitations caused by opening and closing of mechanical relays.

Thermal control of the spacecraft incorporates second surface mirrored radiators to minimize absorbed solar heating and conventional aluminum heatpipes so that heat from electronics and solar absorption can be transported from the sunlit side of the spacecraft to the shadowed side. The suitability of the final thermal design approach will be verified by testing the SSTA structure as described earlier. The sub-structural model would be equipped with representative heaters and MLI, then placed in a small thermal vacuum chamber for testing. This brief test would measure temperature gradients under quasi-steady conditions and provide an estimation of design sensitivities. The results of this test would be used in conjunction with tests performed on the flight PSS at fixed, stable temperatures in air to verify that the measured thermal distortions at various levels are not larger than predicted.

Thermal vacuum testing of the integrated SIM space vehicle would verify that thermal interface requirements have been satisfied, the spacecraft thermal design meets all temperature control requirements, and that thermal hardware performance (heater operation, heatpipe operation, MLI performance) are all within specification. A key to successful performance of integrated thermal system testing is adequate design and thermal testing of the sub-scale PSS wing.

Thermal math models will be created to provide a preliminary assessment of thermal stability. Thermal models, prepared using TSS (Thermal System Solver) and a double precision version of SINDA, will be used to predict transient responses to various thermal disturbances. Thermal analyses performed to date have shown that it is feasible to control temperature excursions of optical elements to less than 2 millikelvin over a one-hour period with an insulated enclosure employing approximately 50 independently controlled heater plates with on/off deadbands of 0.2 K. Thermal stability of the PSS is readily achievable to less than 0.5 K with approximately 10 heater zones per wing with control deadbands of 1.0 K or below. The number of heater zones and the on/off setpoints are key parameters for further optimization of enclosure designs for each application.

7. Key Dynamic Issues

Vibration stability requirements on the PSS were recently 18 micro-g for frequencies below 100 Hz and 0.44 nm/(the number of light bounces)$^{1/2}$ above 100 Hz. System trades will evaluate various combinations of isolation and damping to identify the most cost-effective solution.

Reaction wheel isolation will employ flight-qualified Chandra Observatory isolators. A passive device using six visco-elastic (VEM) damped titanium springs in a hexapod supports each wheel individually. The Chandra Observatory isolator used 9 Hz springs with 10% damping. Near ideal isolation performance was obtained from 10 to 180 Hz. The design can be softened somewhat for SIM requirements. Quiet reaction wheels (much quieter in higher harmonics than the Hubble wheels) will be operated at a minimum spin rate of 600 rpm to avoid the isolator resonance.

Structural damping can be applied throughout the structure using VEM layers on panels or struts and damped joints at latch locations, and mechanically advantaged damping layers using graphite standoffs. Another option is actively enhanced passive isolation, demonstrated by a TRW/JPL team on the SIM Micro Precision Interferometer (MPI) testbed in 1998. The active/passive isolator employed PZT force sensors and voice coil actuators, allowing enhanced isolation from 1-100 Hz.

Microdynamics requirements will be an important design driver for the SIM package. Because of dimensional stability requirements, the PSS structure will consist of bonded GFRP components. Although this construction should be an insignificant source of microdynamic disturbances, this structure will also have inherently low damping (i.e. on the order of 0.1% in the frequency range of interest). TRW has developed a method for increasing damping at the order of magnitude level by bonding GFRP constraining layers to the structure with VEM. The weight and cost impact of this approach, however, must be traded against options for reducing microdynamic sources (e.g. rigidizable hinges and latches), against options for reducing vibrational inputs, such as a second isolation stage; and against other energy absorption options such as dampers in the latches.

8. Conclusions

SIM challenges JPL and its industrial partners to develop an affordable mission with several orders of magnitude improvement in performance over previous missions. This challenge will be met using a judicious combination of existing designs and new technology. Performance and affordability must be balanced with a cost-conscious systems engineering approach to design and implementation trades. The concepts presented in this paper represent the initial steps in making SIM a reality, and illustrate the processes used to date to meet the demanding requirements of space-based interferometry.

9. References

[1] Peter Kahn, "Space Interferometry Mission: A Systems Perspective," *2000 IEEE Aerospace Conference*, March, 2000.

10. Biographies

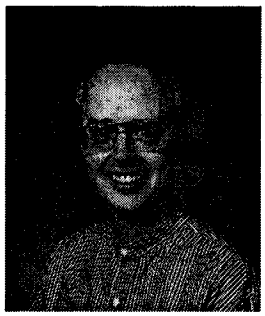

Kim Aaron is a Mechanical Spacecraft Design Engineer. He has worked on the SIM project for almost three years. During his 14-year tenure at JPL, he has been involved in the conceptual design phase of about thirty different space missions. On a recent project, he designed and flight-qualified a vibration isolation system to operate at 2 kelvin for a superfluid helium experiment. Earlier, he was responsible for hardware design, fabrication and assembly of portions of the Rocky 4 microrover, predecessor to the Mars Pathfinder Soujourner rover. In 1985, he graduated from Caltech with a Master of Science and PhD in Aeronautics. He earned a Bachelor of Engineering degree in Honors Mechanical Engineering from McGill University in Montreal, Canada in 1979.

Dave Stubbs is a Mechanical Engineer, leading an Opto-mechanical Engineering group at the Lockheed Martin Missiles and Space Advanced Technology Center in Palo Alto, CA. He has been involved with the SIM program for almost two years, this past year as the LMMS Starlight Lead. During his 20 years at LMMS, he has been involved in all phases of mechanical design; conceptual studies through design analysis and hardware. Previous assignments range from optical brassboards and airborne instruments to conceptual spacecraft studies and satellite instrument flight hardware. He graduated in 1976 from the Florida Institute of Technology in Melbourne, Florida with a Bachelor of Science in Mechanical Engineering and has taken graduate studies at Santa Clara University.

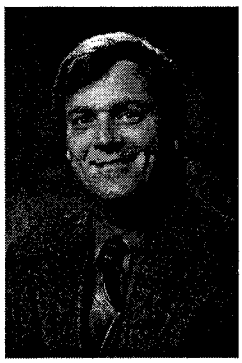

Keith Kroening is the spacecraft systems and mechanical design lead at TRW. He has worked on the SIM project for three years. During his 14-year tenure with TRW, he has supported over twenty conceptual design studies with spacecraft configuration. He was the Mechanical Design Integration lead for the build of a set of DSP early warning satellites, bus layout designer for the Chandra X-ray observatory and the NASA EOS mission. Prior to joining TRW he worked as a Space Shuttle processing engineer with Lockheed supporting 10 launches with the on-board electronics group after moving from Lockheed's Burbank facility where he worked on low observable activities. In 1985, he graduated from the University of Southern California with a BS in Aerospace Engineering where he first plied his space trade on sounding rocket instrument packages to provide background data in support of the Pioneer 10/11 missions.

ACKNOWLEDGEMENT

The work described in this paper was performed under a contract with the National Aeronautics and Space Administration. The work was performed jointly at the three organizations of the authors: California Institute of Technology Jet Propulsion Laboratory, Lockheed Martin Missiles & Space, and TRW. The work was performed by many people besides the authors. Their contributions are appreciated, but it is impractical to list all their names. The painting, commissioned by the SIM project, was painted by Phil Weisgerber. Several of the CAD drawings were prepared by Kevin Jakel of TRW and Buck Holmes of LMMS.